Journal of Theoretical and Applied Information Technology
XX February 20XX. Vol.No.XX

ISSN: 1992-8645 www.jatit.org E-ISSN: 1817-3195

A SURVEY ON THE VEIN BIOMETRIC RECOGNITION SYSTEMS: TRENDS AND CHALLENGES

MOHAMMED SABBIH HAMOUD AL-TAMIMI

Department of Computer Science, College of Science, University of Baghdad, Baghdad, Iraq.
E-mail: m_altamimi75@yahoo.com

ABSTRACT

Vascular patterns were seen to be a probable identification characteristic of the biometric system. Since then, many studies have investigated and proposed different techniques which exploited this feature and used it for the identification and verification purposes. The conventional biometric features like the iris, fingerprints and face recognition have been thoroughly investigated, however, during the past few years, finger vein patterns have been recognized as a reliable biometric feature. This study discusses the application of the vein biometric system. Though the vein pattern can be a very appealing topic of research, there are many challenges in this field and some improvements need to be carried out. Here, the researchers reviewed the different research papers in this area, determined the strengths and weaknesses of these studies, investigated the various improvements made in this fields and the drawbacks which have to be resolved.

Keywords: *Vein, Biometric, Recognition, Vein Features, Vein Pattern.*

1. INTRODUCTION

Veins present in the human subcutaneous tissue, which are hidden beneath the skin, have been described in Figure 1. This is a very reliable and secure biometric feature and is seen to be significant for many reasons:

Firstly, finger veins are an internal characteristic which cannot be faked. Also, it is difficult to change the venous shape and structure of a person. Every individual has distinctive veins, and even identical twins show a different venous pattern [1].

Secondly, the veins get formed during the early embryonic development stages and remain stable throughout a person's life. Unlike the fingerprints, the veins are unaffected by various skin conditions like infections, dehydration, pigmentation anomalies, thick epidermis, or even first or second-degree burns. This shows that the vein patterns are very stable and powerful. In Table 1, the researchers have summarized and compared the different biometric processes.

Figure 1: Angiogram of the Hand Describing the Vascular Network [2]

Table 1. Comparison of the Different Biometric Methods [3]

Biometrics Method	Accuracy	Cost	Size of Template	Long term stability	Security level
Facial Recognition	Low	High	Large	Low	Low
Iris Scan	High	High	Small	Medium	Medium
Finger Print	Medium	Low	Small	Low	Low
Finger Vein	High	Medium	Medium	High	High
Voice Recognition	Low	Medium	Small	Low	Low
Lip Recognition	Medium	Medium	Small	Medium	High

In their study, El-abed *et al.* (2014) [4] described the ideal biometric features, which displayed the following characteristics: (a) Universality, wherein the people are identified based on that feature; (b) Uniqueness; (c) Permanency, wherein the specific feature was stable throughout the person's lifetime;

Journal of Theoretical and Applied Information Technology
XX February 20XX. Vol.No.XX

ISSN: 1992-8645 www.jatit.org E-ISSN: 1817-3195

(d) Collectability, where the feature is obtained from the people without causing any discomfort; and (e) Acceptability, wherein the specific biometric feature is universally accepted and applied to real life. Table 1 described the different venous patterns which satisfy all the above-mentioned characteristics and are considered as an ideal biometric method.

2. TYPE OF BIOMETRIC READING DEVICES:

The finger veins are not visible to the naked human eyes under normal illuminating conditions. On the other hand, they could be viewed using the Near-InfraRed (NIR) light between the wavelengths of 700 and 1000 nm. The human tissues are seen to absorb the NIR light waves, however, these waves get blocked by the deoxidised Haemoglobin (HbO) molecule, which is present in higher concentrations in the human veins, which make these veins darker in the acquired images [1]. The vein-scanners generally support the NIR light waves, which are generated from the Light Emitting Diodes (LEDs), and the Charge Coupled Device (CCD) cameras or the Complementary Metal-Oxide Semiconductor (CMOS) cameras. These devices capture the images of the veins from a particular region. Also, these devices comprise of several optical filters which scatter the NIR-emitted beams and also, increase the contrast of the captured raw images, as described in Figure 2.

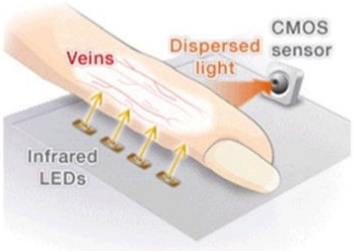

Figure 2: Biometric Imaging Systems for Identifying the Finger Vein Pattern [5]

The vein-reading devices have particular specifications which are as essential as the different processing algorithms which are applied in the finger-vein recognition systems. A high-quality vein scanning device helps in the subsequent image processing. Some of the important factors that affect the final captured image are the sensitivity of the camera to the IR light, the LED system and their arrangement [6]. The design of a vein reader has been described in Figure 3.

Figure 3: A Finger Vein Reader from Hitachi [1]

The hand vein readers have a similar functionality and general concept as the finger vein readers, except that they are larger in size (Figure 4). Moreover, the palm and the dorsal venous network describe the venous of a lower intricacy compared to the finger readers. However, all these techniques are non-invasive, hygienic, and contactless and can be used easily by the public.

Figure 4: A Palm Vein Scanners [1]

Images captured from the vein reading devices are grey-scale and based on the capture devices, could have a compromised image quality. Some additional factors which affect the device specifications include bad illumination, finger orientation, low contrast, environment, shaded areas, and such other factors which decrease the image quality and introduce noise in the image. Generally, if the image quality is not optimal, one cannot carry out feature extraction, matching and recognition, hence; the images are pre-processed or enhanced for improving their quality. The researchers have described the various techniques for solving the problems below.

3. DATA SET:

Datasets are an important component of any vein recognition system. They comprise of images acquired from various individuals with the help of

ISSN: 1992-8645 www.jatit.org E-ISSN: 1817-3195

some scanning devices. The vein biometric dataset includes images of the dorsal hand veins, the palm veins and the finger veins. Examples of different datasets are presented in Figures 5, 6 and 7. However, the technology used for the production of the vein capture devices has not been standardised since this field is new and not investigated in much detail. Every scanning device has different specifications and results in images of varying quality. These datasets are also not available globally for research purposes due to the confidentiality concerns [1]. Different databases are presented in Tables 2, 3 and 4. Fortunately, the vein patterns are easily synthesised with the help of vein generating algorithms, which can generate synthetic venous patterns rather than obtaining them from people. These synthetic vein images are used for training and testing the various biometric systems [7].

Table 2. Various Finger Vein Datasets

Data Set	Availabl	No. of Subjects	Parts scanned per subject	No. of Sessions	No. of Images	Image Size	Device	Year
Hitachi Res. Lab.	NO	2,673	Li;m,Ri;m	1	117, 612	-	TS-E3F1	2004
Int. Biom. Group	NO	650	Li;m,Ri;m	2	28,600	-	TS-E3F1	2006
Hitachi-Kyushu	NO	506	Ri	1	1,012	-	TS-E3F1	2007
PKU v.2,3,4	YES	5,208	Li;l,Ri;l	1	50,700	512× 384	Proto PKU	2008
GUC45 [8]	NO	45	10	12	10,800	512× 240	Proto GUC	2009
SDUMLA-HMT [9]	YES	106	Li;m;r ,Ri;m;r	1	3,816	320× 240	Proto Wuhan Univ.	2010
HKPU[10]	YES	156	Li;m,Ri;m	2	6,264	513× 256	Proto HKPU	2011
UTFVP[11]	YES	60	Li;m;r ,Ri;m;r	1	1,440	672× 380	Proto Twente Univ.	2013
MMC BNU 6000 [12]	YES	100	Li;m;r ,Ri;m;r	1	6,000	640× 480	Proto Chonbuk Univ	2013
CFVD [10]	YES	13	Li;m;r ,Ri;m;r	2	1,345	640× 480	Proto Shandong Univ.	2013
Shandong Uni.	NO	34	Li;m,Ri;m	2	4,080	320× 240	Proto Whuan Univ.	2013
FV-USM [10]	YES	123	Li;m;r ,Ri;m;r	2	5,904	640× 480	Proto Sains Univ.	2013
VERA[11]	YES	110	Li ; Ri	1	440	665× 250	Proto Twente Univ.	2014
MMC BNU 2 [13]	YES	109	Li,m; Ri,m	1	6,976	480× 640	Portable device with two cameras, Chonbuk Nation Univ.	2014

Table 3. Palmar and Dorsal Vein Datasets

Data Set	Availabl	No. of Subjects	Parts scanned per subject	No. of Sessions	No. of Images	Image Size	Device	Year
VERA [14]	YES	110	Lp;Rp	2	2,200	480× 680	Univ. of Applied Sciences Western Switzerland (HES-SO)	2015
PUT Palmar Vein pattern data set [15]	YES	50	Lp,w;Rp,w	3	1,200	1280× 960	-	-
NCUT [16]	YES	102	Ld;Rd	-	2,040	640× 480	-	-
CASIA-MS-PalmprintV1[14]	YES	100	Lp;Rp	2	7,200	768× 576	self-designed multiple spectral imaging device	-
Bosphorus Hand Vein Data Set [17]	YES	100	Ld;Rd	4	1,575	300×240	WAT-902H2 ULTIMATE	2010
GPDS100VeinsCCDcylindrical [17]	YES	102	Rd	2	1,020	-	CCD gigabit Ethernet PULNIX TM3275 camera	2009

ISSN: 1992-8645 www.jatit.org E-ISSN: 1817-3195

Table 4. Wrist Vein Datasets

Databases	Availabl	No. of Subjects	Parts scanned per subject	No. of Sessions	No. of Images	Image Size	Device	Year
PUT Wrist Vein pattern database [15]	YES	50	Lp,w;Rp,w	3	1,200	1280×960	-	-
UC3M [8]	YES	29	Lw;Rw	1	348	640×480	-	2010

Where in all pervious tables: R refers to Right, L refers to Left, i=index, m=middle, r=ring, l=little finger, w=wrist, p=palm, d=dorsal, Li=Left index, Lm=Left middle, Lr=Left ring, Rw=Right wrist, Lp=Left palm, and Ld=Left dorsal.

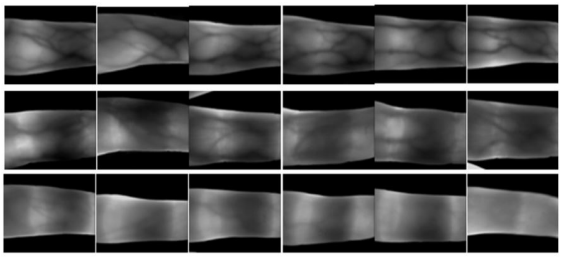

Figure 5: Finger Vein Images Derived from An MMCBNU 6000 Dataset [12]

Figure 6: Raw Palm Vein Images Derived from A VERA Palm Vein Dataset [13]

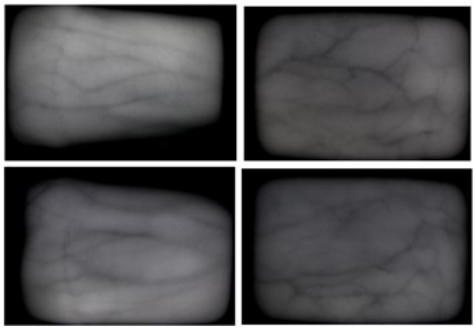

Figure 7: Raw Wrist Veins Images Derived from the PUT Dataset [14]

Furthermore, a few of the researchers created their own specific dataset rather than testing their processes against the popular and standard datasets. However, this could jeopardise the integrity of their results as the data was acquired from a controlled environment wherein the researcher completely controlled the whole enrolment process, right from subject selection, to the type of equipment used, illumination and the no. of scans carried out for every subject. However, the results obtained from these datasets are seen to lack reliability and uniformity, and hence, cannot reflect the full extent of the techniques used or whether the said method could be adopted for public usage. For comparing and assessing the performance of different algorithms, the algorithms are tested against some standard and popular vein databases. This was also suggested by Vanoni *et al.* (2014) [10], who introduced two public datasets. Out of these, one dataset is called VERA, a very challenging dataset that comprises of 440 index fingers images acquired from 110 individuals in an uncontrolled environment. The second is a controlled dataset known as the UTFVP, developed by the University of Twente. The images from the two datasets were acquired with the help of an open device that was developed by the University of Twente.

4. COMMON METRICS USED FOR EVALUATING THE PERFORMANCE OF THE BIOMETRIC SYSTEMS:

The reliability and applicability of a biometric system are based on its performance ability. Evaluating this performance is a complex process since many variables affect the system's performance. In their study, El-abed *et al.* (2014) [4] stated that the performance of these systems is evaluated based on three broad categories; 1) Data quality; 2) Usability, and 3) Security. These three categories are further subdivided into subcategories, as shown in Figure 8.

Journal of Theoretical and Applied Information Technology
XX February 20XX. Vol.No.XX

ISSN: 1992-8645 www.jatit.org E-ISSN: 1817-3195

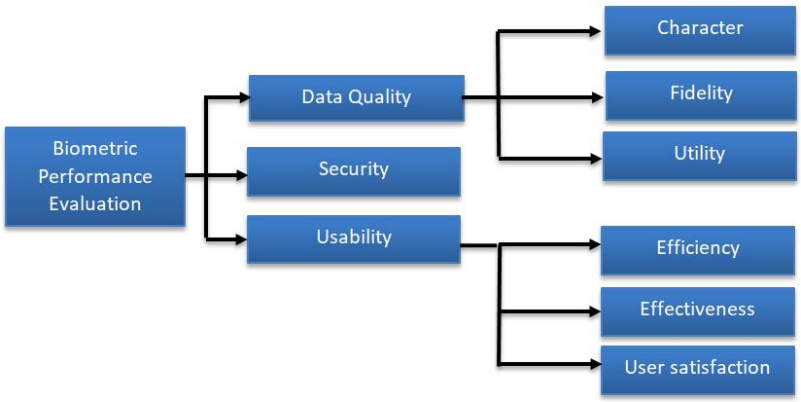

Figure 8: Different Categories for Evaluating the Performance of Biometric Systems

• The quality of the raw data is based on a) Character that refers to the quality of the physical characteristics in a specific individual b) Fidelity that refers to the similarities between the source and the sample images; c) Utility refers to the impact of one sample on the performance of the whole system.

• The security of the whole system is vital. The biometric system has to endure all types of attacks and maintain a reasonable security.

• The usability of the biometric system is also measured based on the a) Efficiency- This refers to the user's capability to complete all tasks rapidly; b) Effectiveness- This indicates if the user is able to use this system effortlessly c) user satisfaction- This describes the overall experience that a user experiences while using the biometric system.

Some general metrics are applied for evaluating the performance of the biometric systems based on the subcategories described in Figure 8 as follows:

4.1 Failure-To-Enrol rate (FTE):
This refers to the ratio of the total no. of successful individual enrolments to the no. of failed enrolments.

4.2 Failure-To-Acquire rate (FTA):
This refers to the ratio of failed attempts for locating or capturing good quality images.

4.3 False-Non-Match Rate (FNMR):
This refers to two samples which are erroneously matched negatively.

4.4 False-Match-Rate (FMR):
This refers to two samples which are erroneously matched positively.

4.5 False Rejection Rate (FRR):
This refers to the probability that an actual sample is rejected by the biometric system and is measured as:

$$FRR(\tau) = FTA + FNMR(\tau) * (1 - FTA) \quad (1)$$

4.6 False Acceptance Rate (FAR):
This refers to the probability that a fake image gets rejected by biometric system and is measured as:

$$FAR(\tau) = FMR(\tau) * (1 - FTA) \quad (2)$$

4.7 Receiver Operating Characteristic curve (ROC):
Refers to a graph wherein the X-axis represents the ratio of the FMR and the FAR, while the Y-axis shows the ratio of FNMR and FRR.

4.8 Equal Error Rate (EER):
This refers to the point of intersection between the FAR and the FRR. The nearer the value of EER to 0, the better is the performance of the biometric system.

4.9 Identification Rate (IR):
This describes the ratio of the total no. of accurate identification attempts to the no. of all the identification attempts.

4.10 False-Negative Identification-error Rate (FNIR):
This is measured as:

$$FNIR(\tau) = FTA + (1 - FTA) * FNMR(\tau) \quad (3)$$

4.11 False-Positive Identification-error Rate (FPIR):
This is measured as:

$$FPIR = (1 - FTA) * (1 - (1 - FMR)^N) \quad (4)$$

ISSN: 1992-8645 www.jatit.org E-ISSN: 1817-3195

4.12 Cumulative Match Characteristic curve (CMC):

This refers to the graph that describes the relationship between the ranks on the X-axis and the IR with a higher or lower rank present on the Y-axis.

5. LITERATURE REVIEW:

5.1 Hands (Palms and Dorsal Veins):

The finger vein images should be of a good quality to enable recognition. Hence, they have to be pre-processed for improving their quality. The pre-processing of the images is carried out using the following set of procedures: (1) Filtering, (2) Resizing, (3) Segmentation, and (4) Thinning [18]. In their study, Ding et al. (2005) [19] suggested the application of a conditional thinning process with a novel threshold for the segmentation procedure. They applied a median filter for de-noising, followed by a feature point distance technique for image matching after estimating the distance between the end and the crossing points in the veins. After comparing their results to those by Tsinghua University, the researchers noted that their results were better and the results are presented in Tables 5 and 6.

Table 5. Ratio of Refusing the Identification

No. of samples	Matching times	No. of passes	Refusing times	Pass ratio (%)	Refusing ratio (%)
240	120	119	4	99.1	0.9

Table 6. Ratio of Mistaken Identity

Number of samples	Matching times	Mistaken times	Mistaken identifying ratio (%)
240	1000	0	0

Image identification is a process where the palm print and the finger vein images for the same person are compared for proving their identity. The ratio of refusing the identification denotes the number of failed identification attempts to the number of total identification attempts. On the other hand, the ratio of mistaken identity compares a single palm print of an individual against all the images present in the data set.

In another study, Ladoux *et al*. (2009) [20] applied the Scale-Invariant Feature Transform (SIFT) descriptor for verifying the hand vein patterns. In Step 1, they cropped the image to obtain a Region of Interest (ROI) and thereafter applied the (5×5) box filter for decreasing the noise. Then, the Gaussian low-pass filter was applied for balancing and obtaining a uniform illumination. The final image was subtracted from the primary unfiltered ROI, and a grey normalisation was carried out for enhancing the image contrast. The features were extracted using a local threshold with SIFT. The EER value was 0.14% without any post-processing step, whereas a ratio of 0 was noted when the image post-processing was included in the technique. This study highlighted the role played by a post-processing step in enhancing the dissimilarities between the fake and the genuine samples.

Septimiu *et al*. (2010) [21] used a mean filter to decrease the noise in the image, followed by an adaptive threshold operation for binarising the image. Thereafter, they applied a thinning algorithm consisting of 15 rules and 4 additional rules for thinning the diagonal lines. They carried out an optimising algorithm for ensuring that the additional pixels were deleted from the image and a single pixel vein pattern was obtained. The researchers applied many algorithms along with a software platform for algorithm testing known as the VIMAGER with the help of the Borland Delphi 7. Here, the FAR and FRR values were 0.012% and 1.03%, respectively.

Ojala *et al*. (1996) [22] proposed the Local Binary Pattern (LBP) operator, which is a very popular image processing and analysis operator. The general idea was to define the textural features of an image since it represents the images as a group of numerical values. This operator can be applied to the grey-level, binary or RGB images, and is also incorporated into the 3-D images and videos [23]. Many studies investigating the vein pattern recognition system expressed interest in the LBP operator, while some other researchers modified and altered this operator to create their own version, which will be discussed later.

Wang *et al*. (2012) [24] designed the feature coding which was based on the Back Propagation (BP) neural network. In this technique, initially, the researchers extracted the rectangular ROI from a hand dorsal vein image after estimating the image centroid, which was followed by the grey- level normalisation and application of a median filter for decreasing the noise. The features of the vein in the image ROI were then divided into 64 rectangular regions, where every region was converted to a

ISSN: 1992-8645 www.jatit.org E-ISSN: 1817-3195

binary sequence after applying the Partition Local Binary Pattern (PLBP) technique. Some features like the Error Correcting Coding (ECC) are inputted into the BP encoders for decreasing the error rate, while the orthogonal gold code was a resultant output. The gold code refers to a sequence which decreases the similarities between the classes. The recognition rate of 97.60% was used along with a combination encoder and a correlation classifier, as a matching technique for the 1000 images.

Lee (2012) [25] applied Otsu's thresholding and a border tracing algorithm for extracting the palm contours. Thereafter, they applied a 2D Gabor filter, which was a textured filter for effectively extracting the palm vein features. This Gabor filter was used in the spatial and the frequency domains. The researcher also developed a novel directional coding process for transforming the vein features to the bit strings known as a VeinCode, for increasing the speed of the matching and recognition techniques. The researchers used a normalised Hamming distance for the VeinCode matching. They tested this technique against the database comprising of 4140 palm vein images acquired from 207 subjects. They noted a recognition rate of >99% and an EER of 0.4%, which proved that the method was robust.

Wu *et al.* (2012) [26] applied a low pass filter along with a binarisation method and extracted the image ROI after determining the Wrist Side Maximal Inscribed Circle (WSMIC), with a radius of RA, while A was the tangent point with a thumb outline and a point. The WSMIC centre was O. thereafter; they connected the points A and O to obtain the AO line. Then, they drew a square wherein the AO line would dissect the square in a half, which represents the ROI (Figure 9).

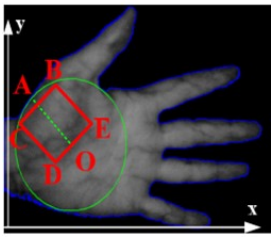

Figure 9: ROI Area Described by ABEODC Within the WSMIC Circle [26]

The features were extracted using the Partial Least Square (PLS) and the wavelet decomposition techniques. The researchers evaluated the performance of their method by experimenting on the dataset consisting of 300 palm vein images. They observed a CRR of 99.86%, while the FAR and FRR values were 0.14% and 0.67%, respectively.

Zeng *et al.* (2012) [27] pre-processed the vein images using relative algorithms and applied appropriate filters, and techniques like normalisation, resizing, thinning and segmentation, along with grey-level normalisation (i.e., contrast stretching) for increasing the contrast in the images. The grey-level normalisation was calculated as:

$$N(I,J)=\begin{cases} M_0+\sqrt{\dfrac{V_0(I(i,j)-M)^2}{V}}, I(i,j)>M \\ M_0-\sqrt{\dfrac{V_0(I(i,j)-M)^2}{V}}, I(i,j)\le M \end{cases} \quad (5)$$

Here, I(i,j), M and V represent the grey intensity, mean and the variance, respectively, prior to normalization, whereas N(i,j), M_o and V_o denote the grey intensity, are grey intensity, mean and variance, respectively, after the normalization process.

Furthermore, the image segmentation is determined using the Niblack formula, which is a very effective and simple technique.

$$m(x,y)=\frac{1}{r^2}\sum_{i=x-\frac{r}{2}}^{x+\frac{2}{r}}\sum_{j=y-\frac{r}{2}}^{y+\frac{r}{2}} f^2(i,j) \quad (6)$$

$$s(x,y)=\sqrt{\frac{1}{r^2}\sum_{i=x-\frac{r}{2}}^{x+\frac{2}{r}}\sum_{j=y-\frac{r}{2}}^{y+\frac{r}{2}} f^2(i,j)} \quad (7)$$

In the above equations, s(x,y) and m(x,y) denote the variance and the mean, respectively for every (r×r) window. Thereafter, the local threshold was determined for every pixel, as follows:

$$T(x,y)=m(x,y)+k*s(x,y) \quad (8)$$

$$\begin{cases} f(x,y)=255 & f(x,y)>T(x,y) \\ f(xy)=0 & f(x,y)\le T(x,y) \end{cases} \quad (9)$$

It must be noted that the correcting coefficients, i.e., (k) and (r) are selected randomly, which is a major drawback of the Niblack technique. Therefore, Liu (2013) [28] proposed an improved and better version of the Niblack method. One vital step used for vein recognition was thinning. This is because the veins contract and dilate due to many factors like arm orientation, temperature etc., hence;

ISSN: 1992-8645 www.jatit.org E-ISSN: 1817-3195

these factors have to be excluded to obtain accurate results. The Hilditch and the Rosenfeld techniques are used for this purpose [27].

Han *et al*. (2012) [29] applied the textural feature approach. The Gabor filter is a very effective technique for extracting the local features. However, the researchers proposed a variation for developing a better version of this filter. Initially, the vein features are converted to the bit code known as VeinCode and are matched using a template. Thereafter, a normalised Hamming distance was used for measuring the similarities between the 2 VeinCodes. The researchers acquired 4140 palm vein images from 207 people for testing their approach. The results were then compared using the conventional Gabor filter (single or multiple) along with their developed adaptive Gabor filter. The time required for feature extraction for the different filters was 42 ms, 822 ms, and 109 ms, respectively.

Prasanna *et al*. (2012) [30] investigated the different pre-processing techniques like the: (1) Image negative, (2) Histogram equalization, (3) Grey level slicing, (4) Contrast stretching, (5) Sharpening, (6) Laplacian sharpening, and the (7) High boost filtering. They used two hand dorsal vein images for comparing the different methods. Their results indicated that the histogram equalization technique, along with the high boost filter method were better than the other techniques.

Zhu *et al*. (2012) [31] developed and proposed a 2-stage framework, where the first was known as the coarse stage, while the 2nd framework was known as the fine stage. For the coarse classification system, Zhu *et al*. (2012) used a novel technique known as the Thinning Energy Cost (TEC), which exploited the textures and the geometric features of the palm dorsal veins. Image pre-processing had to be carried out, followed by the application of the ROI identification, binarisation, and the thinning algorithms for obtaining the skeletal image of the complete venous network. They recorded the no. of the deleted pixels for every one of the iterations. Finally, they obtained the vectors whose dimensions were represented by the no. of iterations for the thinning algorithm and the elements in the vectors were represented by the no. of deleted pixels after each iteration. This feature vector was applied in the coarse classification technique or the TEC method. Thereafter, the researchers used the improved LBP technique for fusing the textural and the geometric features after assigning the weights which corresponded to the vein pixels (%) in every sub-region of a binary region. Then, they described the geometric features after converting this binary image into a graph, and all similarities between the graphs were determined after computing the distance between the key points after implementing the inexact graph matching technique, wherein slightly differing graphs could be easily matched. The researchers applied this technique based on the distortions observed in the vein graphs in the earlier processes. This technique showed a recognition rate of up to 96.67% for the NCUT (North China University of Technology) dataset.

Zhu *et al*. (2013) [32] proposed a novel segmentation process based on the vein properties like the fact that the veins appeared darker than the surrounding tissues in the NIR, their cross-sectional profiles showed a Gaussian-like shape and they were locally linear. Here, the researchers used a matching filter as a convolutional mask for image enhancement. The veins responded to the filter effectively and appeared more prominent while the surrounding tissues did not properly match the filter and were not properly visible. However, the resultant image is not ideal and a local or global threshold cannot be applied. Hence, the novel technique suggested that the central lines in the veins must be extracted using the local maximal curve since the points present in the central region of the hand dorsal veins showed wide curvatures. Initially, the images underwent morphological operations for connecting the unconnected lines, and thereafter, the researchers applied an appropriate thinning algorithm. The researchers proposed the novel Binary Coding (BC) technique, which was applied to the skeletonised images, followed by the implementation of a novel graph matching technique. They compared the proposed method against the NCUT dataset and noted a recognition rate of 98.53%.

Sheetal *et al.* [33] proposed a novel technique for investigating the pre-processing step in the vein recognition system. In this approach, the researchers applied median and average/ low pass filters to the raw acquired images, and thereafter carried out contrast enhancement using 3 techniques (1) Histogram equalization, (2) Adaptive technique, and (3) Adjusting process. Thereafter, the researchers used mathematical morphological operations like 1) Opening operation-this method added pixels to the object boundaries pixels. The object boundaries had to be smoothened and the smaller objects had to be removed and the overall image quality was maintained. This was expressed using the formula below:

ISSN: 1992-8645 www.jatit.org E-ISSN: 1817-3195

$$XoB = (X \ominus B) \oplus B \quad (10)$$

1) Wherein X represents a specific image, while B refers to an object which must be subtracted from X, $\ominus$ represents erosion and $\oplus$ represents dilation.

2) Closing operation- This thinned the object boundaries and filled the gaps present in the object. It was expressed as follows:

$$A.B = (A \oplus B) \ominus B \quad (11)$$

Wherein A referred to a binary image and B was the object. The researchers used the adaptive thresholding process for separating the foreground (i.e. veins) image features from the background. This study helped in obtaining better palm vein images with distinctive extracted features that could be used in the subsequent classification steps.

In another study, Jhinn *et al*. (2015) [34] proposed a new Zig-Zag Valley Detection Algorithm (Z2VDA), which could detect the valley points present in the fingers. These valley points would be used for correcting the hand rotation. In Step 1 of this method, the researchers applied the OTSU threshold for the image binarisation. In Step 2, they used a canny edge detector for extracting the contours present in the palm shape, which helped in obtaining the circular intersection. The circular intersection refers to the intersection between the fingers and a circle, and the centre of the circle was present in the palms of the individual. This proposed algorithm helped in removing the inaccurate intersection points, and hence, only the correct intersection points would be used for calculating the valley points using the Z2VDA algorithm. The researchers observed that they could effectively detect the palm veins in 8 different rotatory angles of 0º, 45º, 90 º, 135º, 180º, 315º, 270º and 255º.

Huange (2015) [35] developed and proposed a novel hand dorsal vein recognition system which compared the local vein features with multiple sources. The researchers did not only focus on the venous network but also considered the surrounding tissue properties and applied their geometric characteristics, unlike other studies. Initially, the image was enhanced using Gaussian filters. Thereafter, a Hessian–Laplace detector was used for identifying the venous features, while a Harris–Laplace detector and a Difference of Gaussian (DoG) technique were used for detecting the geometric characteristics of the skin. They also computed the Oriented Gradient Maps (OGMs) of the primary images for obtaining enhanced and clear geometric characteristics of the images. Finally, they used the SIFT key points for extracting the feature vectors from the above-mentioned OGM gradients, which helped in identifying the features for matching and determining the extent of similarity. The researchers carried out experiments using the NCUT dataset. Their results indicated that this method was efficient and very robust.

Zhang *et al*. (2016) [36] investigated the dorsal hand patterns, unlike the other studies which only concentrated on the local-based processes. The researchers proposed a novel technique for the dorsal vein recognition with a global graph model, which focused on the texture and the shape of the dorsal finger veins. The construction of the graph model was categorised into different steps. In Step 1, the researchers developed a basic graph model, which consisted of a limited minutiae vein network (known as vertices). In Step 2, they developed a detailed graph model which increased the no. of vertices, while the other graph-based studies only focused on the shape. Here, the researchers embedded even the textural details into the graph model. They noted that the application of a holistic approach without textural features led to a recognition rate of 98.82% while the use of a local approach including textural features led to a recognition rate of 99.22%. The researchers carried out their experiments using an NCUT dataset. In Table 7, a comparison between the various holistic techniques and other standard processes has been presented.

Table7: Comparison of the Holistic Approach and Other Methods

Approaches	Recognition rate (%)
Multi-source keypoint + SIFT [35]	99.61
Multi-level keypoint + SIFT [31]	98.04
OGMs + SIFT [37]	99.02
LCP [21]	90.88
LBP + Graph [31]	96.67
BC + Graph [32]	98.53
Detailed Graph Method with holistic features	98.82
Detailed Graph Method with local and holistic features	99.22

Lu *et al*. (2015) [38] proposed a hypergraph matching or a high-order depth-based graph matching process, which was better than their 1st-order depth-based matching process. The 1st-order depth process determined the depth-based vertices that were the point coordinates. A similarity matrix was developed based on the distance between the point coordinates for every vertices pair (representing the matrix elements) and the matching

ISSN: 1992-8645 www.jatit.org E-ISSN: 1817-3195

kernel, which determines the similarity of pairs. Then, a high-order matching process was used for detecting the mismatches arising from this technique.

Unar *et al*. (2014) [39] reviewed the various biometric systems and showed that a combination of the biometrics (i.e., multi-modal biometric systems) generated more accurate results in comparison to the mono-modal systems. However, the type of biometrics implemented for a system must be carefully selected. Based on this approach, Bharathi *et al*. [40] developed and proposed a multi-modal biometric recognition system which used 2 different biometric features, i.e., dorsal and palm veins. Initially, the binarisation technique was used for pre-processing the images. Thereafter, the researchers applied the morphological dilation method for removing the smaller and unconnected objects, along with an average filter for image smoothening. Feature extraction was carried out in 2 steps, i.e., filtering and thresholding. The feature vectors were determined based on the width and location of the veins from the Palm Feature (PF) and Hand Feature (HF) for the palm and dorsal vein images for each person. The PF and HF feature vectors were combined together to form a single Feature vector (F). The researchers determined the similarities using the Euclidean Distance (ED). Also, the False Match Rate (FMR) results indicated that this method was better than a single-modal biometric system.

Wang *et al*. (2017) [41] applied a Gaussian low-pass filter, along with Otsu's thresholding. They used the relative side length that calculated the distance between the middle-index and the pinkie-ring finger valleys, whereas the side length was fixed at 200 pixels, 210 pixels, etc., for extracting the ROI. Thereafter, the researchers used the K-means and a Maximal Principle Curvature (MPC) method for extracting the features, followed by the LBP and template matching processes. The EER values for the template matching process with a relative side length of 1.6d was 0.01965%; while it was 0.058% for the LBP matching process with a relative side length of 1.5d. The researchers experimented on a CASIA v1.0 dataset.

Ali *et al*. (2017) [42] used a Competitive Valley Hand Detection (CHVD) method for ROI extraction. Thereafter, they extracted the features using one of the 3 approaches; LBP, 2D-Local Binary Pattern (2DLBP), or a combination (LPB and 2DLBP) that included the features from these approaches. The researchers applied the Principal Component Analysis (PCA) feature reduction technique and selected the features using the Liner Discrimination Analysis (LDA) method. Experiments were carried out using the CASIA palm print database for determining the similarity scores with ED. They observed 98.55% accuracy after the application of the 3rd process (LBP+2DLBP). Though this novel combination approach was used on the palm prints, the researchers believed that it could provide accurate results for vein patterns.

5.2 Finger Veins:

The earlier studies focused on the palm and dorsal hand veins. In this section, the researchers have investigated the finger vein-based studies. The finger veins differed from the dorsal and palm veins in many ways. From the biological perspective, the finger veins differed from the palm and dorsal veins with regards to their shape, width, size, no. and type of bifurcations. Additionally, the dorsal and the palm templates had a larger dimension than the finger template. The finger vein datasets carried out multiple scans for every individual since a minimum of 2-3 fingers from every hand were scanned for each person. The no. of scans per person played a vital role in the general performance of the method, the processing time required, and the accuracy of the results obtained. Subsequently, for eliminating all differences, the researchers have to use specifically tailored techniques for satisfying all requirements. After observing the results, the researchers stated that the palm and the dorsal systems showed a higher accuracy rate and better results. Some of the studies which investigated the finger vein recognition system are described below.

During the initial development stages of the vein recognition technique, Miura *et al*. (2004) [43] carried out feature extraction based on the dark line-tracking method. This refers to a cross-sectional vein profile which describes the Gaussian-like shape and despite changes in the illumination, still presents a prominent valley shape of the pixel distribution pattern. The line tracking is initiated at any one pixel and the selected pixel is known as the 'current tracking point' that moves at the rate of one pixel at a time and showed that the pixels were of a dark (low) grey intensity. Line tracking is an iterative method with multiple 'current tracking points' to ensure that the complete vein pattern gets scanned. The no. of times the pixel is scanned gets recorded into one matrix known as the locus space. In the feature extraction method, the researchers examined the locus space for determining the pixels that were scanned frequently since they represented

ISSN: 1992-8645 www.jatit.org E-ISSN: 1817-3195

a vein and were of a darker shade. For improving the performance, the researchers suggested decreasing the no. of current tracking lines and the locus space dimensions. The mismatch ratios are shown in Table 8.

Table 8: Mismatch Ratios Between the Conventional and Proposed Methods

Image	Mismatch ratio	
	Proposed method	conventional method
Image(1)	33.5%	47.0%
Image(2)	33.3%	40.3%

Zhang *et al*. [44] developed and proposed a multi-scale feature extraction technique for determining the curvelet-based finger-vein pattern. In step 1 of this technique, the researchers applied a curvelet discomposing step for all the images. This was followed by the self-adaptive adjustment step based on the transform function, which considered the curvelet values. After the curvelet enhancement step, the researchers constructed a local interconnection neural network along with a receptive field and trained it with the RPROP algorithm. They used 2 kinds of samples for training, i.e., (1) A positive training sample which was used when a vein was detected in the 4th column of the subsequent region and showed an output of +1 and (2) A negative training sample with an output of -1. This neural network could only detect the horizontal lines which would help it detect the other lines when the neural network's receptive field was rotated by a value of α. Finally, a template matching technique was applied and the researchers experimented on the 3200 images, i.e., images for 8 fingers each of the 400 volunteers, and an EER value of 0.128% was observed.

However, Chengbo *et al*. (2008) [45] used a novel approach that was inspired by the fuzzy theory. In Step 1 of their technique, they used a twice-coarse segmentation method which classified the image into 3 parts, i.e., (1) Object; (2) Background; and (3) a fuzzy component. The fuzzy component was enhanced using an enhancing algorithm and was further divided. Based on the cross-section of the pixel intensities for a vein, the researchers observed that a valley was formed and hence they applied a feature extraction algorithm for detecting the valley areas and their market directions. Thereafter, the market directions were divided further into 8 components and a method was designed, known as the concave detection algorithm for estimating the convolutions within the 8 directions. The researchers used a multi-threshold segmentation method for tackling the above-mentioned 3 components, separately. The noise from the fuzzy components was decreased and segmented with the help of the regional threshold technique for obtaining a precise feature extraction despite the low image quality. Smooth and accurate results were noted.

Liu *et al*. (2007) [46] aimed to detect the lines despite their width. Hence, they developed a 2-D line detection model which used grey-scale images with circular nonlinear masks. These masks collected the pixels with a brightness equivalent to the mask's central pixel and assembled into a similar brightness-weighted mask.

The earlier studies focused on eliminating the width factor for obtaining accurate results for a vein recognition system. However, in their study, Huang *et al*. (2010) [47] used the vein width data and developed a technique based on that by Liu *et al*. [46]. Huang *et al*. developed a wide line detecting technique, which focused on the extraction of good features from low-quality images. This technique also detected the veins without applying the thinning method. The wide line detector considered several parameters, which can be calculated as follows:

$$N(x_0,y_0)=\left\{(x,y)\middle|\sqrt{(x-x_0)^2}+(y-y_0)^2\le r\right\} \quad (12)$$

$$V(x_0,y_0)=\begin{cases}0 & and\ m(x_0,y_0)<g\\ 255 & and\ otherwise\end{cases} \quad (13)$$

$$m(x_0,y_0)=\sum_{(x,y)\in N_{(x_0,y_0)}} s(x,y,x_0,y_0,t) \quad (14).$$

$$s(x,y,x_0,y_0,t)=\begin{cases}0, & and\ F(x,y)-F(x_0,y_0)>t\\ 1, & and\ otherwise\end{cases} \quad (15)$$

Wherein, F refers to a raw image; V was a feature image and the pixels within the image had a value of either 0 or 255. $N(x_0,y_0)$ was the circular neighbourhood with a radius r, while $f(x_0, y_0)$ was a specific pixel within the raw image and the values of r, t and g were set manually. Thereafter, the researchers used a template generation and conventional template-matching technique. All experiments were carried out on 50,700 images in the database. The researchers concluded that this method showed accurate results for low-quality images. Table 9 compares the EER values for the wide line method, the curvature method and the line-tracking method.

ISSN: 1992-8645 www.jatit.org E-ISSN: 1817-3195

Table 9: Comparison of the EER Values for the Wide Line, Line Tracking and the Curvature Methods

	Line Tracking	Curvature	Wide Line Detector
Without Normalization	6.14%	3.86%	2.86%
With Normalization	5.00%	2.80%	0.87%

Shaohua *et al*. (2012) [48] proposed the application of SIFT for solving the rotation-based problems, wherein they applied the Sobel edge detection to the raw images and obtained the rectangular ROI boundaries. They also implemented the Histogram equalization process for enhancing the contrast between the surrounding tissues and the veins. Feature extraction and data matching were carried out using the SIFT technique since it was rotation and scale invariant. They experimented with three different databases, wherein the first was rotated by ±1º; the second was rotated by ±3º, while the 3rd dataset was rotated by ±5º. The EER values for the 3 datasets were seen to be 2.15%, 2.98%, 2.75%, respectively, whereas the mean EER was 2.63%.

Liu (2013) [28] implemented the adaptive overall threshold process for separating the ROI wherein the average grey-scale values for the vein image were seen to be the threshold. This step was followed by combining the different linear filters, i.e., the Wiener filters for suppressing the Gaussian noise. Though the Weiner filter suppressed the Gaussian noise, it did not significantly affect the salt-pepper noise. This was decreased by the application of the median filter. Finally, the researchers used a grey linear stretch for enhancing the image contrast.

$$g(x,y) = \frac{d-c}{b-a}[f(x,y)-a]+c \quad (16)$$

Wherein f(x, y) was the primary image and g(x, y) represented the stretched image. Meanwhile, [a,b] and [c,d] were the new and old grey limits, respectively.

However, this technique showed a blurred effect, since it used two de-noising filters. The researchers used an improved Niblack process for segmenting and extracting the image features. They developed the equations for determining the r and k coefficients in the Niblack window rather than selecting them randomly. This technique generated better results compared to the original Niblack process. The below equations determine the r coefficient:

$$sum1 = \sum_{x=1}^{m}\sum_{y=1}^{n} f(x,y) \quad (17)$$

$$del = \frac{\sum_{x=1}^{m}\sum_{y=1}^{n}(f(x,y)-sum1)^2}{m \times n} \quad (18)$$

$$t = [del/sum1] \quad (19)$$

$$k = -\log\left(\frac{nj}{ni+1}\right) * 0.05 \quad (20)$$

Wherein; m referred to the average grey values; $f^{*r}max$ were the maximum pixels in the *r*r* window, while $f^{*r}min$ were the minimal number of pixels in the *r*r* window.

As mentioned in this study, several researchers used similar pre-processing techniques, especially in the case of thinning. For skeletonising the image, it should be binarised initially. However, this technique is not always beneficial. Couprie *et al*. (2013) [49] suggested that a thinning technique could be directly applied to the grey-scale images, and hence they proposed a parallel thinning algorithm that could be implemented on the 2D and the 3D images. The researchers stated that this additional step could be implemented before the binary thinning step as it preserved additional details and offered a richer space before transforming them into a black and white space. Furthermore, this technique could also be applied to the grey scale images like the fingerprints [50], medical images [51],[52], and for character recognition [53].

Shahrimie *et al*. [54] proposed a method which combined the finger vein features and the finger geometry. Firstly, the researchers located the finger outline using a (3×3) Laplacian mask, which improved the finger's edges, followed by the Canny edge detector and a rotation alignment that decreased the rotation problems during the scans. They detected the horizontal point, Y_{ft}, and the vertical fingertip points, X_{ft}, after determining the centre point for the distance present between the edge of the fingertips, i.e., X_l and X_r. The researchers drew a vertical line from the vertical point based on the mean X values along the right and left finger edges. The Δy value was set at 380 pixels and the rotation was determined as:

$$\tan\theta = \frac{\Delta x}{\Delta y} = \frac{X_{ft}-X}{Y_{ft}-Y} \quad (24)$$

The researchers carried out finger vein feature extraction using the Band-Limited Phase-Only Correlation (BLPOC) and the Width-Centroid

ISSN: 1992-8645 www.jatit.org E-ISSN: 1817-3195

Contour Distance (WCCD) function for determining the finger's geometrical features. Finally, they used the score-level fusion for integrating the finger veins and the finger geometry features. An EER value of 1.78% was noted when they used their own dataset for experimentation.

Rosdi *et al*. (2011) [55] implemented the Local Line Binary Pattern (LLBP) process, based on the LBP process for feature extraction. This technique showed a better performance compared to the LBP and the Local Derivative Pattern (LDP) processes. They used a novel capturing device with a modified camera and an IR-LED, at a wavelength of 880nm. They also used an open window with a fixed size (2.5cm×2.5cm) for reducing the rotation-induced effects during image capture. They applied the Otsu's method for image pre-processing during image binarisation, and the image was cropped to a final size of 480×160. For feature extraction, the LBBP technique consisted of the horizontal and vertical components. The LLBP magnitude is based on the sum of the line binary codes in these components. After extracting the features, they are compared using the following formula for Hamming Distance (HD):

$$HD = \frac{\|codeA \otimes codeB\|}{CodeLength} \quad (25)$$

The *codeB* was the primary code and code A refers to the extracted binary code, while the CodeLength refers to the length of the overall enrolled codes. They experimented on their dataset for determining the optimum length of line N along with the filter S size. LLBP was used for optimal matching, where the length of line (N) was 21 and the filter mask (S) size was 15. Using the LLBPv technique, the optimal values for N and S were seen to be 17 and 15. All results have been presented in Tables 10 and 11.

Table 10: EER Values (%) by Varying the N and S in the LLBP Process with a Sub-Dataset for Finger Vein

N	S	11	13	15	17	19
17		3.33	2.11	2.11	2.78	2.67
19		3.22	2.11	2.11	2.56	2.56
21		3.22	2.11	1.89	2.56	2.56
23		3.22	2.11	1.89	2.56	2.33
25		3.22	2.00	1.89	2.44	2.33

Table 11: EER Values (%) by Varying the N and S in the LLBPv Process with a Sub-Dataset for Finger Vein Images (N: line length; S: size of the filtering mask)

N	*S*	11	13	15	17	19
13		3.11	2.33	1.89	2.44	2.33
15		3.11	2.03	1.89	2.33	2.22
17		3.00	2.00	1.78	2.33	2.22
19		3.00	2.00	1.78	2.22	2.17
21		2.89	2.00	1.78	2.22	2.12

Setitra *et al*. (2015) [56] applied the SIFT operator for classifying and matching the images. This operator was generally applied to the textured images. Their technique helped in extracting the outline of the shapes in the monochromatic images. The SIFT approach, applied to the binary images, showed better results than its application on the grey or RGB images. These findings could help in investigating the grey-scale vein images. This study highlighted the significance of the binarisation process in the pre-processing of venous images.

Xian *et al*. (2015) [57] developed a novel Recognition Algorithm Test Engine (RATE) system for evaluation. The algorithms, which had to be investigated, were uploaded to the system using a web application and the results were rapidly generated. This system consisted of three parts; 1) Database 2) View and benchmark management tools and 3) A distributed computation system. The researchers used the Peking University dataset, which consisted of 110000 images (i.e., 25 samples/ finger). Table 12 shows the classification of this dataset into other subsets. The management tools provided similarity scores and values for the FRR, FAR and other metrics like EER, FMR etc. Lastly, the distributed computing system operated on the 32-bit window clusters and decreased the processing times for the submitted algorithms. Though this technique allowed multiple submissions by the participants, only one of these submissions would be investigated. The participants could use the OpenCV library. Table 13 presents the ranking results for the algorithms.

Table 12: Datasets Used in the RATE System

Dataset	Size	Released	Description
DS0	10×5	Yes	For quick debug
DS1	944×5	No	Volunteers
DS1-	100×5	Yes	Subset of DS1
DS2	1000×5	No	Real application
DS2-	100×5	Yes	Subset of DS2
DS3	1000×5	No	Synthetic set
DS3-	100×5	Yes	Subset of DS3

ISSN: 1992-8645 www.jatit.org E-ISSN: 1817-3195

Table 13: Ranking of the Submitted Algorithms

Rank	No.	EER (%)	Author (s)	Note
1	A13	0.375	A-Eye	Industry
2	A16	1.32	Anonymous	Industry
3	A1	3.545	FY. Jin	Academia
4	A3	3.875	JX. Yu	Academia
5	A2	5.59	N. Wang	Academia
6	A9	9.451	Y. Guo *et al.*	Academia
7	A7	19.665	Anonymous	N/A

Many researchers used graph matching in the biometric systems for image recognition. Earlier studies observed good results and a low EER value of 0.5% when the Biometric Graph Matching (BGM) technique was used for the retina vein recognition. Hence, Nibbelke (2015) [58] used this technique for finger vein recognition. In this technique, 2 different graphs are compared to one another based on the similarities between the graph edges. Since the raw images already show imperfections, the researchers increased the image contrast to decrease the noise that could affect the system reliability. They selected the BGM technique as it was noise tolerant. After image enhancement, the researchers carried out a thinning process and reduced the noise further. Thereafter, the vein skeleton was converted into a graph, which was represented as; g= (V, E, μ, v) wherein, V refers to the vein features (e.g., crossovers, bifurcation, and termination), E refers to the connected pair of branches, and μ: V $\rightarrow R^2$ converted every value of v to its corresponding Cartesian coordinates (q1, q2). The researchers applied a greedy RANSAC process for ensuring that the graphs were aligned properly and were rotation free. All experimentation was carried out using the UTwente finger vein image database and an EER value of 0.93% was seen after the researchers used only 10% of this dataset. This EER value increased to 2.89% after they used 40% of this dataset. Hence, the researchers concluded that this BGM technique was not very effective for finger vein recognition as they obtained very different results compared to the standard methods.

Dong *et al.* (2015) [11] proposed the Difference Symmetric Local Graph Structure (DSLGS) technique for finger vein recognition. They obtained the feature values based on the information for the position, gradient information, and the weights of the edges multiplied by the corresponding difference coefficient pixels. An LDA technique was used for reducing the dimensionality. Thereafter, the K Nearest Neighbour (k-NN) classifier was used for matching where k =1. Experiments were carried out on the MMCBNU 6000 Database.

Table 14: Comparison of the EER Values for the Proposed and Standard Methods

Algorithms	LBP	LGS	SLGS	DSLGS
EER (%)	4.87	5.22	5.72	3.28

In [59], the researchers stated that feature extraction was the backbone for any biometric recognition system and could significantly affect the accuracy and processing speed of the end recognition. The researchers implemented the Contrast-Limited Adaptive Histogram Equalizations (CLAHE) technique after the ROI extraction. They also used the Niblack algorithm for image binarisation. Furthermore, they applied the morphology thinning algorithm having a dilation operation for skeletonising the binarised image and also decreasing the noise. The researchers stated that though some of the blocks within the image did not have any vein pattern, they were still useful. All experiments were carried out using the MMCBNU 6000 and MMCBNU 2C datasets. Finally, they used a histogram intersection technique for measuring the similarities between the histograms as described below:

$$D(h_A, h_B) = \sum_{g=0}^{P-1} \min(h_A(g), h_B(g)) \quad (26)$$

In a recent study, Vasquez et al. (2017) [60] determined the geometric properties for the finger vein features and thereafter proposed a novel technique that relied on the hybrid curves and used a Hough transform. The ROI was extracted using a Sobel filter, while the contours in the veins were extracted using the Canny Algorithm. The Hough transform refers to a line detection algorithm that detects the lines which can fulfil the line equations and help in extracting the lines from the binarised images. The researchers divided the complete parametric space into cells, followed by the evaluation of the line equation for pixels within the final image. The equation was satisfied after the pixels satisfied the condition that the cell no. must increase by 1, which showed that the cell was likely to be a vein line. The researchers used the SDUMLA-HTM dataset, which consisted of data from 106 individuals (i.e., 6 images for the middle, index and the ring fingers for both the hands). The results showed that this was a robust feature extraction method and could be used in the later stages of the biometric system. However, the results

ISSN: 1992-8645 www.jatit.org E-ISSN: 1817-3195

are based on the segmentation strategy used and could vary if the conditions are changed.

Qin *et al*. (2017) [61] used a deep Neural Network (NN) method and proposed a novel deep learning model which could be used for the finger-vein verification. This technique helped in predicting the likelihood of a pixel being a vein or a background pixel, after labelling every pixel position foreground as or background based on the human knowledge. Thereafter, the foreground (vein) pixels were segmented from the background. This technique used the statistics of the nonlinear pixel correlations for segmenting and recovering the lost vein pattern. The researchers also proposed a Convolutional Neural Network (CNN)-based technique for automatically detecting the features from the raw pixels. This CNN approach consisted of different layers like finger vein labelling, CNN building, training and testing of the CNN, and feature encoding. The EER value was seen to be 1.33% after the template matching. Experiments were carried out on two datasets, where, one used a contactless device, i.e., the finger-vein database from the Hong Kong Polytechnic University, which consisted of 3132 images acquired from 156 individuals. The 2nd dataset used a contact device, i.e., the Universiti Sains Malaysia (USM) database which consisted of 5904 images.

Waluś *et al*. (2017) [62] investigated the acquisition device, specifically the effect of the NIR spectrum on the acquired vein image quality. The researchers developed a novel device having varying wavelengths, which could acquire 11556 vein images from 107 different subjects. This device used 9 NIR wavelengths for image capturing (i.e., 730 nm, 808 nm, 850 nm, 860 nm, 875 nm, 880 nm, 890 nm, 940 nm and 950 nm). Their experiments determined a link between the selection of an appropriate wavelength and the image identification performance using this biometric system. Researchers observed that the wavelength of 875 nm was the most ideal and the biometric systems showed 99.4% accuracy at this wavelength.

CONCLUSION:

In this study, the researchers have investigated the advantages and disadvantages of the different techniques used in the biometric recognition systems. This study also described the suitability of these techniques for different applications. Many novel hybrid processes could be developed based on the concepts presented in this study. Furthermore, this study also highlighted the important datasets that could be used by the biometric recognition system. Many earlier studies had investigated the palm and the dorsal hand veins in detail; however, the finger vein identification systems need to be investigated further. Furthermore, better software and hardware techniques have to be developed for studying the actual potential of a finger vein biometric system.

In most papers reviewed, it was found that they follow the same pattern. For preprocessing, most studies utilized some sort of preprocessing method, and while preprocessing is a crucial part of any system, it largely depends on the condition of the data. However, extensive preprocessing and filtering may not be always a necessity. In fact, over preprocessing can cause undesirable results where some valuable details may be lost in the process especially when working on extracting textured features in veins. Some of the steps in the papers discussed can be optional such as binarization, and thinning processes. In feature extraction, most studies focused on utilizing texture features for vein recognition since it offered the most satisfactory results. Furthermore, most of the studies focused on using local features. Local features proved to be far more optimum than holistic approaches. For matching and recognition phase, template matching and distance such as chi-square or Euclidean distance were very common methods. Finally, it was noted that very little work was done to test the robustness of the vein biometric against fraud or imposter attacks. Hence, imposter vein prints need to be further studied. Additionally, there's only few large, and publicly available datasets for research purposes. Therefore, there is a need for more publicly available datasets to help researchers and help us to get more uniform, reliable results.

REFRENCES:

[1] Crisan S. Biometric Security and Privacy. Jiang R, Al-maadeed S, Bouridane A, Crookes PD, Beghdadi A, "Biometric Security and Privacy". *Cham: Springer International Publishing*; 2017, pp. 21-50. (Signal Processing for Security Technologies).

[2] Sos TA, Trost D. "Peripheral angiography : Medica Mundi", vol. 41, No. 2 , pp. 36–42, 1997.

[3] Saini, R., Narinder, R., "Comparison of Various Biometric Methods", *International Journal of Engineering Science and Technology*, vol.2, No. I, pp. 24–30, 2014.

[4] El-Abed M, Charrier C, Rosenberger C. "Evaluation of Biometric Systems. In: New

ISSN: 1992-8645 www.jatit.org E-ISSN: 1817-3195

Trends and Developments in Biometrics". *InTech*; pp. 149–69, 2014.

[5] Valavan TT, Kalaivani MR. "Biometric Authentication System Using Finger Vein", vol. , pp. 50-55.

[6] Crisan S, Tarnovan IG, Crisan TE. "Vein Pattern Recognition, Image Enhancement and Feature Extraction Algorithms". vol. 5, 2007.

[7] Hillerström F, Kumar A, Veldhuis R. "Generating and Analyzing Synthetic Finger Vein Images". *Biosig*. 2014;

[8] Pflug A, Hartung D, Busch C. "Feature Extraction from Vein Images Using Spatial Information and Chain Codes". *Information Security Technical Report*. vol. 17, no. (1–2), pp. 26–35, 2012.

[9] Yin Y, Liu L, Sun X. "SDUMLA-HMT: A Multimodal Biometric Database". *In: Lecture Notes in Computer Science (including subseries Lecture Notes in Artificial Intelligence and Lecture Notes in Bioinformatics)* . pp. 260–8, 2011.

[10] Vanoni M, Tome P, El Shafey L, Marcel S. "Cross-Database Evaluation Using An Open Finger Vein Sensor". *In: 2014 IEEE Workshop on Biometric Measurements and Systems for Security and Medical Applications (BIOMS) Proceedings . IEEE*; 2014. pp. 30–5.

[11] Dong S, Yang J, Wang C, Chen Y, Sun D. "A New Finger Vein Recognition Method Based on the Difference Symmetric Local Graph Structure (DSLGS)". *International Journal of Signal Processing, Image Processing and Pattern Recognition*. vol. 8, no. 10, pp. 71–80, 2015.

[12] Park DS, Yoon S, Lu Y. "Finger Vein Identification System Using Two Cameras". *Electronics Letters* . vol. 23;50, no. 22, pp.1591–1593, 2014.

[13] Tome P, Marcel S. "Palm Vein Database and Experimental Framework for Reproducible Research". *In: 2015 International Conference of the Biometrics Special Interest Group (BIOSIG). IEEE*; 2015 [cited 2017 Nov 11]. pp. 1–7.

[14] Das A, Pal U, Ballester MAF, Blumenstein M. "A New Wrist Vein Biometric System". *In: 2014 IEEE Symposium on Computational Intelligence in Biometrics and Identity Management (CIBIM). IEEE*; 2014. pp. 68–75.

[15] Kumar TA, Premalatha K, Natarajan AM. "Hand Vein Pattern Recognition Using Natural Image Statistics". *Defence Science Journal* . vol. 21, no. 65(2), pp.150–8, 2015.

[16] Trabelsi RB, Masmoudi AD, Masmoudi DS. "A New Multimodal Biometric System Based on Finger Vein and Hand Vein Recognition". *International Journal of Engineering and Technology*. vol. 5, no. 4, pp. 3175–3183, 2013.

[17] Yang J, Shi Y, Yang J. "Finger-Vein Image Restoration Based on a Biological Optical Model". *In: New Trends and Developments in Biometrics*. pp. 59–72, 2012.

[18] Ahmed M. A., Ebied HM, El-Horbaty EM, Salem A. M. "Analysis of Palm Vein Pattern Recognition Algorithms and Systems". *Journal of Bio-Medical Informatics and e-Health*. vol. 1, no. 1, pp. 10-14, 2013.

[19] Ding YDY, Zhuang DZD, Wang KWK. "A Study of Hand Vein Recognition Method". *IEEE International Conference Mechatronics and Automation*. vil. 4, pp. 2106–2110, 2005.

[20] Ladoux PO, Rosenberger C, Dorizzi B. "Palm Vein Verification System Based on SIFT Matching". *Lecture Notes in Computer Science (including subseries Lecture Notes in Artificial Intelligence and Lecture Notes in Bioinformatics)*. 5558 LNCS: pp.1290–1298, 2009.

[21] Crisan S, Tarnovan IG, Crisan TE. "Radiation Optimization and Image Processing Algorithms in the Identification of Hand Vein Patterns". *Computer Standards and Interfaces*. vo. 32, no. 3, pp 130-140, 2010.

[22] Ojala T, Pietikäinen M, Harwood D. "A Comparative Study of Texture Measures With Classification Based on Featured Distributions". *Pattern Recognition* . vol. 29, no. 1, pp. 51-59, 1996.

[23] Pietikäinen M, Hadid A, Zhao G, Ahonen T. "Computer Vision Using Local Binary Patterns". *London: Springer London*; 2011. (Computational Imaging and Vision; vol. 40).

[24] Techniques R. "Lecture Notes in Computer Science" . Vol. 4536, Lecture Notes in Computer Science. 2012.

[25] Lee JC. "A Novel Biometric System Based on Palm Vein Image". *Pattern Recognition Letters* . vol. 33, no. 12 pp. 1520-1528, 2012.

[26] Wei Wu, Wei-qi Yuan, Jin-yu Guo, Sen Lin, Lan-tao Jing."Contact-Less Palm Vein Recognition Based on Wavelet Decomposition and Partial Least Square". *Biometric Recogntion,7th Chinese Conference Proceedings(CCBR)*, Vol. 4536 ,pp. 176–183, 2012.

[27] Zeng X, Jin W. "Research of Hand Vein Patterns Recognition for Biometric

ISSN: 1992-8645 www.jatit.org E-ISSN: 1817-3195

Identification". *Proceedings - 2012 International Conference on Biomedical Engineering and Biotechnology, iCBEB 2012.* 2012, pp. 884–887.

[28] Liu C. "A New Finger Vein Feature Extraction Algorithm". *In: 2013 6th International Congress on Image and Signal Processing (CISP) . IEEE*. 2013, pp. 395–399.

[29] Han WY, Lee JC. "Palm Vein Recognition Using Adaptive Gabor Filter". *Expert Systems with Applications*. vol. 39, no. 18, pp. 13225-13234, 2012.

[30] Deepak PR, Neelamegam P, Sriram S, Nagarajan R. "Enhancement of Vein Patterns in Hand Image for Biometric and Biomedical Application Using Various Image Enhancement Techniques". *Procedia Engineering*. vol. 38, pp. 1174-1185, 2012.

[31] Xiangrong Zhu and Di Huang,"Hand Dorsal Vein Recognition Based on Hierarchically Structured Texture and Geometry Features", *Biometric Recogntion,7th Chinese Conference Proceedings(CCBR)*, vol. 4536, pp. 157–164, 2012.

[32] Zhu X, Huang D, Wang Y. "Hand Dorsal Vein Recognition Based on Shape Representation of the Venous Network". *Lecture Notes in Computer Science (including subseries Lecture Notes in Artificial Intelligence and Lecture Notes in Bioinformatics)*. 8294 LNCS, pp. 158–169, 2013.

[33] Goela RP, Garg K. "Image Processing in Hand Vein Pattern Recognition System". *International Journal of Advanced Research in Computer Science and Software Engineering*. 2014;4(6):427–30.

[34] Jhinn WL, Kah G, Michael O, Connie T, Hui LT. "For Contactless Palm Vein Biometrics". *In: 3rd International Conference on Information and Communication Technology (ICoICT)*. 2015, pp. 568–573.

[35] Huang D, Tang Y, Wang Y, Chen L, Wang Y. "Hand-Dorsa Vein Recognition by Matching Local Features of Multisource Keypoints". *IEEE Transactions on Cybernetics*. vol. 45, no. 9 pp. 1823-1837, 2015.

[36] Zhang R, Huang D, Wang Y. "Textured Detailed Graph Model for Dorsal Hand Vein Recognition : A Holistic Approach". *In: International Conference on Biometrics*. 2016.

[37] Huang D, Tang Y, Wang Y, Chen L, Wang Y. "Hand Vein Recognition Based on Oriented Gradient Maps and Local Feature Matching". *Lecture Notes in Computer Science (including subseries Lecture Notes in Artificial Intelligence and Lecture Notes in Bioinformatics)*. 7727 LNCS(PART 4), pp. 430–444, 2013.

[38] Lu Bai, Zhihong Zhang, Peng Ren, Edwin R. Hancock, "A High-Order Depth-Based Graph Matching Method", *Computer Analysis of Images and Patterns*, *G. Azzopardi and N. Petkov (Eds.), part I, 16th International Conference, CAIP,* vol. 1296, Valletta, Malta, 2015, pp. 465–476.

[39] Unar JA, Seng WC, Abbasi A. "A Review of Biometric Technology Along With Trends and Prospects". *Pattern Recognition*. vol. 47, no. 8, pp. 2673–2688, 2014.

[40] S.Bharathi, R.Sudhakar. "Biometric Recognition Using Dorsal and Palm Vein Images". *International Journal of Advanced Engineering Technology*. vol. 4, no. 2, pp. 415-419, 2016.

[41] Wang P, Sun D. "A Research on Palm Vein Recognition". *International Conference on Signal Processing Proceedings, ICSP*. pp. 1347–1351, 2017.

[42] Ali MMH, Yannawar PL, Gaikwad AT. "ScienceDirect Multi-Algorithm of Palmprint Recognition System Based on Fusion of Local Binary Pattern and Two-Dimensional Locality Preserving Projection". *Procedia Computer Science*. vol. 115, pp. 482–492, 2017.

[43] Miura N, Nagasaka A, Miyatake T. "Feature Extraction of Finger-Vein Patterns Based on Repeated Line Tracking and Its Application to Personal Identification". *Machine Vision and Applications*. vol. 15, no. 4, pp. 194–203, 2004.

[44] Zhongbo Z, Siliang M, Xiao H. "Multiscale Feature Extraction of Finger-Vein Patterns Based on Curvelets and Local Interconnection Structure Neural Network". *Proceedings - International Conference on Pattern Recognition*. vol. 4, pp. 145–158, 2004.

[45] Yu C, Qin H. "A Research on Extracting Human Finger Vein Pattern Characteristics". *Proceedings of the World Congress on Intelligent Control and Automation (WCICA).* 2008, pp. 3783–3788.

[46] Liu L, Zhang D, You J. "Detecting Wide Lines Using Isotropic Nonlinear Filtering". *IEEE Transactions on Image Processing*. vol. 16, no. 6 , pp. 1584–1595, 2007.

[47] Huang B, Dai Y, Li R, Tang D, Li W. "Finger-Vein Authentication Based on Wide Line Detector and Pattern Normalization". *In: International Conference on Pattern*

ISSN: 1992-8645 www.jatit.org E-ISSN: 1817-3195

Recognition Finger-vein. 2010, pp. 1273–1286.

[48] P. Shaohua, Y. Yilong , Y. Gongping, L. Yanan, "Rotation Invariant Finger Vein Recognition", *Biometric Recogntion,7th Chinese conference Proceedings(CCBR), Springer,* 2012, pp. 151–156.

[49] Couprie M, Bezerra N, Bertrand G. "A Parallel Thinning Algorithm for Grayscale Images". *Lecture Notes in Computer Science (including subseries Lecture Notes in Artificial Intelligence and Lecture Notes in Bioinformatics).*7749 LNCS, pp. 71–82, 2013.

[50] Abbood AA, Al-Tamimi MSH, Peters SU, Sulong G. "New Combined Technique for Fingerprint Image Enhancement". *Modern Applied Science*. vol. 11, no. 1, pp. 222-234, 2017.

[51] Al-Tamimi MSH, Sulong G. "Tumor Brain Detection Through MR Images: A Review of Literature". *Journal of Theoretical and Applied Information Technology*. vol. 62, no. 2, pp. 387–403, 2014.

[52] Al-Tamimi MSH, Sulong G. "A Review of Snake Models in Medical MR Image Segmentation". *Jurnal Teknologi (Sciences and Engineering)*. vol. 69, no. 2, pp.101-106, 2014.

[53] Ahmed, A.A., Al-Tamimi, M.S., Al-Sanjary, O.I. and Sulong G. "Classification of Arabic Writer Based on Clustering Techniques". *Fatos Xhafa, Technical University of Catalonia, Barcelona S, editor. Springer;* pp. 48-58, 2017.

[54] Mohd Asaari MS, Suandi SA, Rosdi BA. "Fusion of Band Limited Phase only Correlation and Width Centroid Contour Distance for finger based biometrics". *Expert Systems with Applications.* vol. 41, no. 7, pp. 3367-3382, 2014.

[55] Rosdi BA, Shing CW, Suandi SA. "Finger Vein Recognition Using Local Line Binary Pattern". *Sensors*. vol. 11, no. 12, pp. 11357–11371, 2011.

[56] Setitra I., Larabi S., "SIFT Descriptor for Binary Shape Discrimination, Classification and Matching". *In: Azzopardi G., Petkov N. (eds) Computer Analysis of Images and Patterns. CAIP 2015. Lecture Notes in Computer Science*, vol. 9256. Springer, Cham

[57] Xian R, Ni L, Li W. "The ICB-2015 Competition on Finger Vein Recognition". *In: Biometrics (ICB) 2015 International Conference on*. 2015. pp. 85–89.

[58] Nibbelke V. Vascular "Pattern Recognition for Finger Veins Using Biometric Graph Matching". 2014, pp. 1–13.

[59] Liu BC, Xie SJ, Park DS. "Finger Vein Recognition Using Optimal Partitioning Uniform Rotation Invariant LBP Descriptor". *Journal of Electrical and Computer Engineering*. pp. 1–11, 2016.

[60] Vasquez Y, Beltran C, Gomez M, Florez M, Vazquez-Gonzalez JL. "Features Extraction in Images on Finger Veins With Hybrid Curves". *2017 IEEE Mexican Humanitarian Technology Conference, MHTC 2017*. 2017, pp.34–38.

[61] Qin H, El-yacoubi MA. "Deep Representation-Based Feature Extraction and Recovering for Finger-Vein Verification". *IEEE Transactions on Information Forensics and Security*. vol. 12, no. 8, pp. 1816–1829, 2017.

[62] 62. Waluś M, Bernacki K, Konopacki J. Impact of NIR wavelength lighting in image acquisition on finger vein biometric system effectiveness. Opto-Electronics Revie. 2017;25(4):263–8.